

# Unprecedented Chain-Length-Dependent Conformational Conversion Between 11/9 and 18/16 Helix in $\alpha/\beta$ -Hybrid Peptides\*\*

Baptiste Legrand, Christophe André, Laure Moulat, Emmanuel Wenger, Claude Didierjean, Emmanuel Aubert, Marie Christine Averlant-Petit, Jean Martinez, Monique Calmes,\* and Muriel Amblard\*

**Abstract:**  $\alpha,\beta$ -Hybrid oligomers of varying lengths with alternating proteogenic  $\alpha$ -amino acid and the rigid  $\beta^{2,3,3}$ -trisubstituted bicyclic amino acid ABOC residues were studied using both X-ray crystal and NMR solution structures. While only an 11/9 helix was obtained in the solid state regardless of the length of the oligomers, conformational polymorphism as a chain-length-dependent phenomenon was observed in solution. Consistent with DFT calculations, we established that short oligomers adopted an 11/9 helix, whereas an 18/16 helix was favored for longer oligomers in solution. A rapid interconversion between the 11/9 helix and the 18/16 helix occurred for oligomers of intermediate length.

The development of heterogeneous backbones combining  $\beta$ -amino acids with  $\alpha$ -amino acids has significantly extended the chemical and structural diversity of foldamers.<sup>[1–4]</sup> In recent years, helical secondary structures of  $\alpha,\beta$ -hybrid peptides involving monosubstituted  $\beta^2$ - or  $\beta^3$ -amino acids<sup>[5–8]</sup> and cycloalkyl- $\beta^{2,3}$ -amino acids<sup>[3,4,8–16]</sup> have been well described. The ring-constrained  $\beta$ -amino acids constitute particularly attractive building blocks to generate organized and functionalized  $\alpha,\beta$ -hybrid peptides. Within the family of foldamers containing ring-constrained  $\beta$ -amino acids, unique conformations or conformational polymorphisms have been observed, which were highly dependent on the structure and stereochemistry of the individual building blocks. Indeed, short  $\alpha,\beta$ -hybrid oligomers containing *trans*-2-aminocyclopentanecar-

boxylic acid residues (*trans*-ACPC residues) were able to adopt both the 11 and 14/15 helix.<sup>[9,11]</sup> However, no evidence of a helical fold was found for *trans*-2-aminocyclohexanecarboxylic acid-(*trans*-ACHC)-containing hybrid sequences. Extended conformations were also preferred for oligomers with alternating *cis*-ACHC and L-alanine,<sup>[17]</sup> whereas the corresponding D-alanine-containing sequences that followed the stereochemical patterning approach proposed by Fülöp and co-workers<sup>[14]</sup> adopted a distinct 11/9 helix.<sup>[16]</sup> Unlike cycloalkyl- $\beta^{2,3}$ -amino acid-containing peptides, studies on  $\alpha/\beta$ -hybrid peptides involving hindered  $\beta$ -amino acid residues such as *gem*-disubstituted  $\beta^{2,2}$ - or  $\beta^{3,3}$ -, acyclic disubstituted  $\beta^{2,3}$ -, or trisubstituted compounds, are rather limited. Early work by Seebach et al.<sup>[2,18]</sup> assumed that such residues induce steric hindrances that destabilize the secondary structures of  $\beta$  peptides; as well, it was thought that the unfavorable distribution of substituents in the amide plane might prevent hydrogen bonding. However, a limited set of helical folds with *gem*-dialkyl  $\beta$ -amino acids were recently obtained in combination with the  $\alpha$ -aminoisobutyric (Aib) residue known to be a strong helical inducer. Balaram et al.<sup>[19]</sup> demonstrated that alternating Aib and the achiral cyclohexyl- $\beta^{2,2}$ -amino acid residues resulted in an 11-helical fold in the tetra- and pentapeptide. Another study involving Aib and an acyclic *trans*- $\beta^{2,3}$ -amino acid, which normally promotes an extended conformation in  $\beta$  peptides,<sup>[20]</sup> also described the formation of an 11-helical structure in solution.<sup>[21]</sup>

Herein, owing to the high propensity of the highly constrained  $\beta^{2,3,3}$ -trisubstituted bicyclic amino acid (*S*)-1-aminobicyclo[2.2.2]octane-2-carboxylic acid (ABOC)<sup>[22]</sup> to promote both a reverse turn into peptides<sup>[23]</sup> and stable helix in homo- and mixed oligoureas,<sup>[24]</sup> we investigated its incorporation into peptide sequences (Figure 1).

ABOC combines the structural constraints of both cyclohexyl- and *gem*-dialkyl- $\beta$ -amino acids and thereby exhibits limited range values of  $\phi$ ,  $\theta$ , and  $\psi$  backbone torsional angles. Indeed, it displays a high degree of conservation of the three angles with favorable gauche conformations when incorporated into both the central position of a reverse turn of  $\alpha,\beta$  tripeptides, or when driving helical folding of homo- or mixed oligoureas.<sup>[23,24]</sup> It is noteworthy that the ABOC derivative has the ability to impose an unexpected  $C_\alpha$ - $C_\beta$  synclinal conformation to the adjacent (*S*)- $\beta$ -amino acid derivative promoting the folding in mixed oligoureas. Despite the strong ability of ABOC as helix inducer in oligoureas, its incorporation in oligoamides to drive helical systems has never been explored. Here, we investigated its impact to favor the folding among  $\alpha/\beta$ -hybrid

[\*] Dr. B. Legrand,<sup>[4]</sup> Dr. C. André,<sup>[4]</sup> L. Moulat, Prof. J. Martinez, Dr. M. Calmes, Dr. M. Amblard  
 IBMM, UMR 5247 CNRS, Universités Montpellier 1 et 2  
 15 avenue Charles Flahault, 34000 Montpellier (France)  
 E-mail: monique.calmes@univ-montp2.fr  
 muriel.amblard@univ-montp1.fr  
 Homepage: <http://www.ibmm.univ-montp1.fr>

Dr. M. C. Averlant-Petit  
 LCPM—UMR 7568 CNRS Université de Lorraine  
 1 rue Grandville, 54001 Nancy Cedex 1 (France)

E. Wenger, Dr. C. Didierjean, Dr. E. Aubert  
 CRM2, UMR 7036 CNRS Université de Lorraine  
 Boulevard des Aiguillettes  
 54506 Vandoeuvre-lès-Nancy Cedex (France)

[†] These authors contributed equally to this work.

[\*\*] We thank the CNRS, MESR, ANR (ANR-08-BLAN-0066-01), and the LabEx ChemISyst for financial support, the SCBIM and Université de Lorraine for NMR and XRD facilities. GENCI-CINES is also thanked for providing access to computing facilities.



Supporting information for this article is available on the WWW under <http://dx.doi.org/10.1002/anie.201407329>.

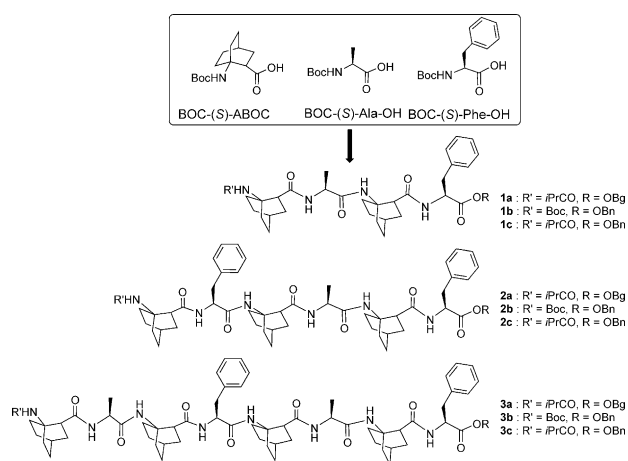


**Figure 1.** Structure of ( $\alpha$ AA-(*S*)-ABOC)<sub>*n*</sub>  $\alpha/\beta$ -hybrid peptides.

peptides with 1:1 proteogenic  $\alpha$ -amino acid ( $\alpha$ -AA)/ABOC residues repeat pattern. We thus prepared hybrid peptides of different length with 1:1 alternation of (*S*)-ABOC and (*S*)-Ala or (*S*)-Phe by stepwise assembly using standard solution Boc/Bn strategy (Figure 1, see the Supporting Information, SI, for full synthesis details). Different capping groups (Boc or *i*PrCO) associated with two types of esters, *N*-benzhydryl-glycolamide ester (OBg)<sup>[25]</sup> and benzyl ester (OBn) were introduced at the N- and C-terminal part of oligomers for crystallization trials.

Whereas attempts to crystallize the oligomers **1a–3a** capped by an *i*PrCO and an OBg group failed, crystals of enantiopure **1c**, **2c**, and **3b** were obtained by slow evaporation of diethyl ether solutions (Figure 2 and Figures S1–S3).

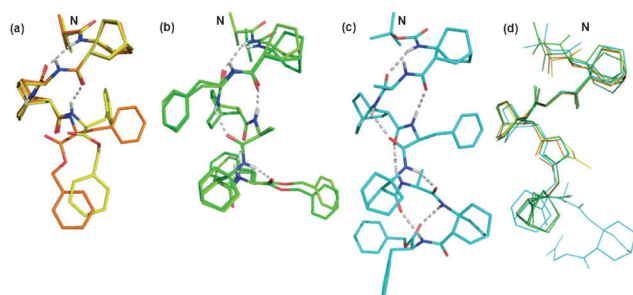


**Figure 2.** Crystal structures of 1:1  $\alpha/\beta$ -hybrid peptides: a) Superimposition of the two independent molecules of tetramer **1c**; b) superimposition of the two independent molecules of hexamer **2c**; c) octamer **3b**. The intramolecular hydrogen bonds are indicated as dashed lines. Hydrogens have been omitted except for the amide protons. d) Backbones superimposition of **1c** (lemon green), **2c** (green), and **3b** (cyan). C-terminal OBn groups have been omitted.

The asymmetric units of tetramer **1c** and hexamer **2c** consisted of two molecules exhibiting similar right-handed mixed 11/9 helix defined by backbone C=O...H–N hydrogen bond forming a C<sub>11</sub> pseudocycle between the CO of the  $\beta$  residue (*i*) and the NH of the  $\alpha$  residue (*i* + 3) and a C<sub>9</sub> pseudocycle between the CO of the  $\alpha$  residue (*i*) and the NH of the  $\beta$  residue (*i* – 1). The superimposition of the two

independent molecules of **1c** (Figure 2a) showed only variations involving the C-terminal  $\alpha$ -amino acid and the OBn moiety. In one crystalline form, the hydrogen bond network was incomplete since the last C<sub>9</sub> pseudocycle between the carbonyl of the Phe residue and the  $\beta$  residue amide proton was disrupted (O...N distance of 4.2 Å) by the incorporation of a water molecule. In contrast, both independent molecules of **2c** exhibited complete hydrogen bond networks (five hydrogen bonds) and displayed only subtle differences.

Octamer **3b** showed a single fully folded 11/9 helix with consecutive alternating eleven- and nine-membered-ring hydrogen bonds in the opposite direction. The overlay of the conformations of tetramer **1c**, hexamer **2c**, and octamer **3b** (Figure 2d) showed that  $\alpha/\beta$  peptides incorporating the ABOC residue adopted a similar 11/9-helical fold from four to eight residues in the solid state with an alternating reverse hydrogen bond pattern *i, i* + 3/*i, i* – 1. The different N-terminal capping groups Boc or *i*PrCO did not influence the helical conformation of such oligomers in the solid state. Although the NMR solution structure of the 11/9 helix was earlier described,<sup>[7]</sup> the detailed structural information was not available until the high resolution structure of alanine/*cis*-ACHC oligomers from crystals of racemic mixtures was recently reported.<sup>[16]</sup> In the family of ABOC-containing oligomers, the enantiopure tetra-, hexa-, and octamer afforded crystals suitable for X-ray diffraction measurements. The average values of the backbone torsion angles for the ABOC residue were  $\phi = 75^\circ$ ,  $\theta = 58^\circ$ ,  $\psi = -91^\circ$  and  $\phi = -70^\circ$  and  $\psi = 164^\circ$  for the  $\alpha$  residue (Table 1). These angle values

**Table 1:** Average backbone torsion angles of 11/9 helices.

Residue	Dihedral angles [°]	( <i>S</i> )- $\alpha$ -AA/ ( <i>S</i> )- $\beta^{2,3,3}$ - ABOC <sup>[a]</sup>	( <i>R</i> )- $\alpha$ -Ala/ (1 <i>R</i> ,2 <i>S</i> )- <i>cis</i> - ACHC <sup>[a],[16]</sup>	( <i>R</i> )- $\alpha$ -AA/ ( <i>S</i> )- $\beta^3$ - acyclic <sup>[b],[7]</sup>	Theoretical studies <sup>[c]</sup>
$\beta$ -AA	$\phi$	75	–87	–94	–77
	$\theta$	58	–52	–60	–60
	$\psi$	–91	97	86	100
$\alpha$ -AA	$\phi$	–70	61	76	60
	$\psi$	164	–151	–142	–150

[a] Crystal structures. [b] NMR solution structures. [c] Average values reported in Ref. [26].

as well as the number of residues per turn and the pitch of about 3.0 and 6.2 Å, respectively, were quite similar to those of the characteristic 11/9 helix reported in other  $\alpha/\beta$  peptides.<sup>[7,16]</sup>

NMR experiments were carried out in chloroform and methanol at a concentration of 5 mM (Figure S5 for <sup>1</sup>H NMR spectra). We observed that modification of the capping groups of oligomers only slightly influenced the resonances and the spectra line widths. Globally, the NMR signals in all series were rather well-dispersed, except for strong overlaps for H<sub>δ</sub> and the H<sub>ε</sub> of the ABOC residues. In contrast, H<sub>α</sub>, H<sub>γ</sub>, and H<sub>ζ</sub> of the ABOC were particularly useful to identify characteristic NOE patterns.<sup>3</sup>*J*(HNH $\alpha$ ) coupling constants of

the  $\alpha$ -amino acids exhibited rather small average values ( $<6$  Hz) in methanol and chloroform for the central residues in hexa- and octamers, which was consistent with  $\phi$  angle values of ca.  $60^\circ$  (Table S13). We detected numerous unambiguous  $i,i+2$ ,  $i,i+3$ , and  $i,i+4$  nonsequential NOEs. Although the  $i,i+2$ ,  $i,i+3$  set of NOEs provided strong evidence that oligomers also adopted an 11/9 helix in solution, the presence of long range  $i,i+4$  NOE correlations for **2a** and **3a** was inconsistent with this conformation and pointed out conformational discrepancies of the  $\alpha$ -AA/ABOC-hybrid peptides in solution and in the solid state. We used ROESY spectra recorded in methanol to further investigate this point. We first assigned NOE sets for compounds **1a**, **2a**, and **3a** bearing *i*PrCO and OBg moieties at their N- and C-terminus, respectively. These correlations were then used as restraints for the NMR solution structure calculations using a simulated annealing protocol with AMBER 11. Tetramer **1a** adopted the 11/9-helical conformation like in the solid state, whereas the longer octamer **3a** converged toward a right-handed 18/16 helix, which was consistent with the  $i,i+4$  NOE patterns (Figures 3 and S20, for mixed helix nomenclature see

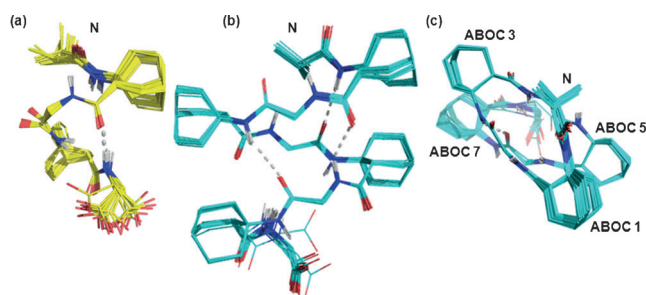


**Figure 3.** The 20 lowest energy NMR solution structures in methanol of the  $\alpha,\beta$  peptides, a) **1a** and b) **3a**. c) Axial view of the NMR structure. Side chains of  $\alpha$  residues, N-terminal OBn group and some hydrogen atoms have been omitted for clarity.

Ref. [7]). This structure is stabilized by two types of intramolecular H bonds forming a  $C_{18}$  pseudocycle between the CO of the  $\beta$  residue ( $i$ ) and the NH of the  $\alpha$  residue ( $i+5$ ) and a  $C_{16}$  pseudocycle between the CO of the  $\alpha$  residue ( $i$ ) and the NH of the  $\beta$  residue ( $i-3$ ) (Figure 3). Interestingly, among the  $\alpha/\beta$ -hybrid octamers, both the 11/9- and 18/16-mixed helices had been predicted by theoretical calculations to be favored structures.<sup>[26]</sup> For hexamer **2a**, numerous distance violations occurred during the simulations. The coexistence of 11/9 and 18/16 helix-typical NOEs suggested a rapid interconversion on the NMR timescale between the two helical folds. The circular dichroism signatures of the oligomers exhibited similar shapes with positive Cotton effects according to their right-handed helical folds. We observed a strong maximum at 205 nm with a shoulder at around 220 nm, which were compatible with the profiles of both types of helices described in the literature<sup>[12,15]</sup> (see SI).

The  $\alpha$ -AA/ABOC 18/16 helix was comparable to that recently determined in solution for the  $\alpha$ -AA/(1*S*,2*R*)-*cis*-ACPC peptides.<sup>[15]</sup> Nevertheless, although the  $\alpha$  residues adopted a similar extended conformation, the torsion angle

**Table 2:** Average backbone torsion angles of  $\alpha/\beta$ -hybrid peptides in the solid state (11/9 helix) and in solution (18/16 helix).

Residue	Dihedral angles [°]	$\alpha$ -AA/ (S)-ABOC (DRX)	$\alpha$ -AA/ (S)-ABOC (NMR) <sup>[a]</sup>	$\alpha$ -AA/ (1 <i>S</i> ,2 <i>R</i> )- <i>cis</i> -ACPC <sup>[15]</sup>
$\beta$ -AA	$\phi$	75	61	108
	$\theta$	58	52	9
	$\psi$	-91	-91	-96
$\alpha$ -AA	$\phi$	-70	-156	-129
	$\psi$	164	174	-176

average values of the  $\beta$  residues were somewhat different, that is,  $\phi = 61^\circ$ ,  $\theta = 52^\circ$ , and  $\psi = -91^\circ$  instead of  $\phi = 108^\circ$ ,  $\theta = 9^\circ$ , and  $\psi = -96^\circ$  (Table 2). These values were imposed by the constrained ABOC motif that displayed a high degree of conservation of its three  $\phi$ ,  $\theta$ , and  $\psi$  angles as observed in the oligourea series.<sup>[24]</sup> It can be noticed that, using the  $\theta$  and  $\psi$  angle conformational space representation of helical  $\alpha,\beta$ -hybrid peptides reported by Balaram et al.,<sup>[4]</sup> the conformational space of the ABOC residue in the 18/16 helix is located in a region devoid of described helical structure so far. The 18/16-helical structure, stabilized by  $i,i-3$  and  $i,i+5$  CO $\cdots$ HN hydrogen bonds, had a number of residue per turn of ca. 4, a rise per turn of ca. 5.0 Å and displayed a large diameter of 7.5 Å compared to 4.0 Å for the 11/9 helix of  $\alpha$ -AA/ABOC peptides and the  $3_{10}$  helix, and to 4.6 Å for the  $\alpha$  helix. The interconversion between the 11/9 and the 18/16 helix involved only a single major structural rearrangement, that is,  $\phi$  angle rotation of  $\alpha$  residues by about  $90^\circ$ . Such conformational equilibrium was not observed by Reiser et al.<sup>[15]</sup> but they did not include  $\alpha/\beta$  oligomers shorter than a 9-mer in their study. Gellman et al.<sup>[11]</sup> reported the chain-length-dependent folding preference among 1:1  $\alpha/\beta$  peptides alternating (S)-Ala, Aib, and (S,S)-ACPC, which interconvert between 11 and 14/15 helix rather than adopting a single hybrid helical conformation. The coexistence in solution of 11- and 14/15-helical conformations for octamers combining (S)-Ala and a *cis*- $\beta$ -sugar amino acid was also described by Jagannadh.<sup>[13]</sup> Furthermore, it is noteworthy that no helical polymorphism was observed neither by the group of Sharma<sup>[5,7]</sup> nor by the group of Choi<sup>[16]</sup> in  $\alpha/\beta$  peptides of different length (trimer to heptamer) promoting 11/9-mixed helices.

In the case of  $\beta$  peptides, such a conformational polymorphism was reported by both Seebach and co-workers<sup>[27]</sup> and Fülöp and co-workers.<sup>[28]</sup> Interestingly, helical polymorphism occurs among  $\alpha$  peptides between the  $\alpha$  and  $3_{10}$  helices depending on the chain length and the solvent polarity.<sup>[29,30]</sup>

To gain more insight into the helix conformational preference of the various series of  $\alpha$ -AA/ABOC-hybrid peptides in methanol and chloroform, diagnostic NOEs were used. We first identified the correlations that were exclusive to each type of helix, from the 11/9 helix crystal structures and the NMR solution structures of the 18/16 helix (Figure 4, Table S15).

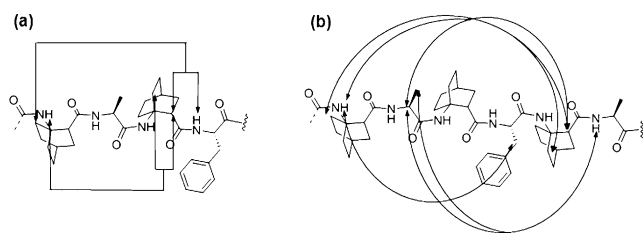


**Figure 4.** Unambiguous nonsequential NOE correlations specific to the a) 11/9 and b) 18/16 helix.

The corresponding NOE peaks localized in rather clear regions of the ROESY spectra were then carefully examined for all oligomers (Figures S6–S22). Four and eight NOEs were identified as useful probes for the 11/9 and the 18/16 helix folding preferences, respectively. For each correlation, a NOE peak was expected for one helix but not for the other one. Typically the characteristic NOEs of the 11/9 helix correspond to interproton distances greater than 5.5 Å in the 18/16 helix, therefore these NOEs could not be found for this helical conformation. Conversely, the typical NOEs of the 18/16 helix were unexpected for the 11/9 helix as the resulting interproton distances were greater than 5.8 Å in this conformation (Table S15). Tetramers **1a**, **1b**, and **1c** exhibited few nonsequential NOEs due to their short lengths and the relative flexibility of the extremities which dramatically affected the NOE intensities. For compound **1a**, three of the four possible characteristic NOEs of the 11/9 helix could be assigned but none of the 18/16 helix. Similar results were found for tetramers **1b** and **1c**, in which only two and one of the four possible typical NOEs of the 11/9 helix were observed, respectively, whereas none of the 18/16-helical conformation was detected. The missing NOE correlations for the 11/9 helix were overlapping or could not be detected. Spectra of hexamers **2a**, **2b**, and **2c** exhibited numerous specific nonsequential NOEs, which could be unambiguously assigned despite overlapping resonances. We detected NOE correlations that were consistent with the two helices indicating that hexamers adopted both the 11/9- and the 18/16-helical conformations in methanol. In contrast, for octamers **3a**, **3b**, and **3c** only typical correlations of the 18/16 helix along the sequences were observed suggesting that they only adopted this conformation in methanol. Studies of compounds **1b**, **2b**, and **3a–3c** in chloroform showed a comparable trend. Only weak NOE correlations specific to the 11/9 helix remained in the ROESY spectra of the octamers suggesting that this helix might be slightly more stable in nonpolar solvents (Figure S22). Thus, it should be concluded that longer  $\alpha$ -AA/ABOC hybrid sequences favor the 18/16 helix relative to the 11/9 helix. To verify this hypothesis, we performed *ab initio* calculations to evaluate the relative stability of the 11/9 versus the 18/16 helix as a function of the oligomer lengths. Both 11/9 and 18/16 structures of the tetra-, hexa-, and octamers were optimized in the gas phase using density functional theory (DFT) calculations. Interestingly, the theoretical calculations were in complete agreement with the NMR studies. The 11/9 fold was clearly more stable than the 18/16 for the tetramer ( $\Delta G = G_{11/9} - G_{18/16} =$

$-28.5 \text{ kJ mol}^{-1}$ ), whereas the 18/16 fold was preferred for the octamer ( $\Delta G = 27 \text{ kJ mol}^{-1}$ ). In the case of the hexamer, comparable free energy values were obtained for the two helices ( $\Delta G = -4.6 \text{ kJ mol}^{-1}$ ) supporting the transition observed in solution (Table S16 and computational details in SI). This type of length-dependent helix preference was already reported for other  $\beta$ - and  $\alpha/\beta$ -hybrid peptides, but also in natural peptides, for which the  $\alpha$  helix is favored over the  $3_{10}$  helix when the number of residues increases.<sup>[29]</sup>

In conclusion, we solved the crystal structures of  $\alpha/\beta$ -hybrid peptides of length ranging from four to eight alternating (*S*)- $\alpha$ -amino acids and (*S*)-ABOC residues. We showed that  $\alpha/\beta$  peptides display an 11/9 helix in the solid state whatever their length, whereas only tetramers were able to adopt a single 11/9 helix in solution. The hexamers adopt both the 11/9 helix and a wider 18/16 helix, which interconvert rapidly. The octamers favor the 18/16 helix in solution, suggesting that in longer  $\alpha$ -AA/ABOC hybrid peptides, the formation of larger hydrogen-bonded rings rather than the formation of a maximum of intramolecular hydrogen bonds minimizes the backbone conformational energy. These results were consistent with the DFT energy calculations that also supported the presence of an unprecedented 11/9 helix and 18/16 helix polymorphism over a preferred 11/9 helix as observed in the solid state. The constraints imposed by the crystal lattice as well as the packing interactions should influence the conformational preference of the  $\alpha$ -AA/ABOC sequence. Altogether these results indicate that length-dependent folding preferences within this family of oligomers should be considered for function-orientated foldamer design. To address this point, the influence of the nature of the  $\alpha$ -amino acid side chains on the helix preference will be also investigated.

Received: July 17, 2014

Published online: September 26, 2014

**Keywords:** 11/9 helix · 18/16 helix · bicyclic  $\beta$ -amino acid · foldamers ·  $\alpha,\beta$ -hybrid peptides

- [1] a) S. H. Gellman, *Acc. Chem. Res.* **1998**, *31*, 173–180; b) R. P. Cheng, S. H. Gellman, W. F. DeGrado, *Chem. Rev.* **2001**, *101*, 3219–3232; c) C. M. Goodman, S. Choi, S. Shandler, W. F. DeGrado, *Nat. Chem. Biol.* **2007**, *3*, 252–262.
- [2] a) D. J. Hill, M. J. Mio, R. B. Prince, T. S. Hughes, J. S. Moore, *Chem. Rev.* **2001**, *101*, 3893–4011; b) D. Seebach, A. K. Beck, D. J. Bierbaum, *Chem. Biodiversity* **2004**, *1*, 1111–1239.
- [3] a) W. S. Horne, S. H. Gellman, *Acc. Chem. Res.* **2008**, *41*, 1399–1408; b) T. A. Martinek, F. Fulop, *Chem. Soc. Rev.* **2012**, *41*, 687–702; c) L. K. A. Pilsl, O. Reiser, *Amino Acids* **2011**, *41*, 709–718.
- [4] P. G. Vasudev, S. Chatterjee, N. Shamala, P. Balaram, *Chem. Rev.* **2011**, *111*, 657–687.
- [5] G. V. M. Sharma, P. Nagendar, P. Jayaprakash, P. R. Krishna, K. V. S. Ramakrishna, A. C. Kunwar, *Angew. Chem. Int. Ed.* **2005**, *44*, 5878–5882; *Angew. Chem.* **2005**, *117*, 6028–6032.
- [6] a) D. Seebach, B. Jaun, R. Sebesta, R. I. Mathad, O. Flogel, M. Limbach, H. Sellner, S. Cottens, *Helv. Chim. Acta* **2006**, *89*, 1801–1825; b) J. D. Sadowsky, J. K. Murray, Y. Tomita, S. H. Gellman, *ChemBioChem* **2007**, *8*, 903–916; c) G. V. Sharma, P. Nagendar, K. V. Ramakrishna, N. Chandramouli, M. Choudhary, A. C. Kunwar, *Chem. Asian J.* **2008**, *3*, 969–983; d) G. V.

- Sharma, N. Chandramouli, S. J. Basha, P. Nagendar, K. V. Ramakrishna, A. V. Sarma, *Chem. Asian J.* **2011**, *6*, 84–97.
- [7] G. Srinivasulu, S. K. Kumar, G. V. M. Sharma, A. C. Kunwar, *J. Org. Chem.* **2006**, *71*, 8395–8400.
- [8] a) J. L. Price, W. S. Horne, S. H. Gellman, *J. Am. Chem. Soc.* **2007**, *129*, 6376–6377; b) G. V. M. Sharma, T. A. Yadav, M. Choudhary, A. C. Kunwar, *J. Org. Chem.* **2012**, *77*, 6834–6848.
- [9] A. Hayen, M. A. Schmitt, F. N. Ngassa, K. A. Thomasson, S. H. Gellman, *Angew. Chem. Int. Ed.* **2004**, *43*, 505–510; *Angew. Chem.* **2004**, *116*, 511–516.
- [10] a) S. De Pol, C. Zorn, C. D. Klein, O. Zerbe, O. Reiser, *Angew. Chem. Int. Ed.* **2004**, *43*, 511–514; *Angew. Chem.* **2004**, *116*, 517–520; b) M. A. Schmitt, B. Weisblum, S. H. Gellman, *J. Am. Chem. Soc.* **2004**, *126*, 6848–6849.
- [11] S. H. Choi, I. A. Guzei, L. C. Spencer, S. H. Gellman, *J. Am. Chem. Soc.* **2008**, *130*, 6544–6550.
- [12] G. V. M. Sharma, N. Chandramouli, M. Choudhary, P. Nagendar, K. V. S. Ramakrishna, A. C. Kunwar, P. Schramm, H. J. Hofmann, *J. Am. Chem. Soc.* **2009**, *131*, 17335–17344.
- [13] B. Jagadeesh, A. Prabhakar, G. D. Sarma, S. Chandrasekhar, G. Chandrashekar, M. S. Reddy, B. Jagannadh, *Chem. Commun.* **2007**, 371–373.
- [14] I. M. Mandity, E. Weber, T. A. Martinek, G. Olajos, G. K. Toth, E. Vass, F. Fulop, *Angew. Chem. Int. Ed.* **2009**, *48*, 2171–2175; *Angew. Chem.* **2009**, *121*, 2205–2209.
- [15] L. Berlicki, L. Pilsl, E. Weber, I. M. Mandity, C. Cabrele, T. A. Martinek, F. Fulop, O. Reiser, *Angew. Chem. Int. Ed.* **2012**, *51*, 2208–2212; *Angew. Chem.* **2012**, *124*, 2251–2255.
- [16] M. Lee, J. Shim, P. Kang, I. A. Guzei, S. H. Choi, *Angew. Chem. Int. Ed.* **2013**, *52*, 12564–12567; *Angew. Chem.* **2013**, *125*, 12796–12799.
- [17] S. H. Choi, M. Ivancic, I. A. Guzei, S. H. Gellman, *Eur. J. Org. Chem.* **2013**, 3464–3469.
- [18] D. Seebach, S. Abele, T. Sifferlen, M. Hanggi, S. Gruner, P. Seiler, *Helv. Chim. Acta* **1998**, *81*, 2218–2243.
- [19] K. Basuroy, V. Karuppiyah, N. Shamala, P. Balaram, *Helv. Chim. Acta* **2012**, *95*, 2589–2603.
- [20] D. Seebach, S. Abele, K. Gademann, B. Jaun, *Angew. Chem. Int. Ed.* **1999**, *38*, 1595–1597; *Angew. Chem.* **1999**, *111*, 1700–1703.
- [21] D. Balamurugan, K. M. Muraleedharan, *Chem. Eur. J.* **2012**, *18*, 9516–9520.
- [22] O. Songis, C. Didierjean, C. Laurent, J. Martinez, M. Calmes, *Eur. J. Org. Chem.* **2007**, 3166–3172.
- [23] C. André, B. Legrand, C. Deng, C. Didierjean, G. Pickaert, J. Martinez, M. C. Averlant-Petit, M. Amblard, M. Calmes, *Org. Lett.* **2012**, *14*, 960–963.
- [24] a) B. Legrand, C. Andre, E. Wenger, C. Didierjean, M. C. Averlant-Petit, J. Martinez, M. Calmes, M. Amblard, *Angew. Chem. Int. Ed.* **2012**, *51*, 11267–11270; *Angew. Chem.* **2012**, *124*, 11429–11432; b) C. André, B. Legrand, L. Moulat, E. Wenger, C. Didierjean, E. Aubert, M. C. Averlant-Petit, J. Martinez, M. Amblard, M. Calmes, *Chem. Eur. J.* **2013**, *19*, 16963–16971.
- [25] M. Amblard, M. Rodriguez, J. Martinez, *Tetrahedron* **1988**, *44*, 5101–5108.
- [26] C. Baldauf, R. Gunther, H. J. Hofmann, *Biopolymers* **2006**, *84*, 408–413.
- [27] a) D. Seebach, J. V. Schreiber, S. Abele, X. Daura, W. F. van Gunsteren, *Helv. Chim. Acta* **2000**, *83*, 34–57; b) X. Daura, D. Bakowies, D. Seebach, J. Fleischhauer, W. F. van Gunsteren, P. Kruger, *Eur. Biophys. J.* **2003**, *32*, 661–670.
- [28] A. Hetényi, I. M. Mandity, T. A. Martinek, G. K. Toth, F. Fulop, *J. Am. Chem. Soc.* **2005**, *127*, 547–553.
- [29] K. A. Bolin, G. L. Millhauser, *Acc. Chem. Res.* **1999**, *32*, 1027–1033.
- [30] M. Bellanda, S. Mammi, S. Geremia, N. Demitri, L. Randaccio, Q. B. Broxterman, B. Kaptein, P. Pengo, L. Pasquato, P. Scrimin, *Chem. Eur. J.* **2007**, *13*, 407–416.